Prashant M. Bapat · Sujata V. Sohoni ·
Tessa A. Moses · Pramod P. Wangikar

A cybernetic model to predict the effect of freely available nitrogen substrate on rifamycin B production in complex media

Abstract It is well-known that secondary metabolite production is repressed by excess nitrogen substrate available in the fermentation media. Although the nitrogen catabolite repression has been known, quantitative process models have not been reported to represent this phenomenon in complex medium. In this paper, we present a cybernetic model for rifamycin B production via *Amycolatopsis mediterranei* S699 in complex medium, which is typically used in industry. Nitrogen substrate is assumed to be present in two forms in the medium; available nitrogen (S_{ANS}) such as free amino acids and unavailable nitrogen (S_{UNS}) such as peptides and proteins. The model assumes that an inducible enzyme catalyzes the conversion of S_{UNS} to S_{ANS}. Although S_{ANS} is required for growth and product formation, high concentrations were found to inhibit rifamycin production. To experimentally validate the model, five different organic nitrogen sources were used that differ in the ratio of S_{ANS}/S_{UNS}. The model successfully predicts higher rifamycin B productivity for nitrogen sources that contain lower initial S_{ANS}. The higher productivity is attributed to the sustained availability of S_{ANS} at low concentration via conversion of S_{UNS} to S_{ANS}, thereby minimizing the effects of nitrogen catabolite repression on rifamycin production. The model can have applications in model-based optimization of substrate feeding recipe and in monitoring and control of fed batch processes.

Introduction

An industrial fermentation process represents a complex chain of subprocesses where a deviation in any one subprocess can adversely affect the productivity (Stanbury and Whitaker 1984). Besides viable and physiologically active biomass (Bapat et al. 2005), fermentation media is an important variable, which decides the fate of the fermentation. The fermentation media components can affect the fermentation process at all stages including seed maturation (Bapat et al. 2003) and production (Bapat and Wangikar 2004). Among these media components, organic nitrogen substrates (S_{ONS}), because of their complex and relatively unknown composition, often become a causative agent for low as well as inconsistent product yield (Calam 1987). These are byproducts of agricultural or animal processes; examples include defatted soy flour (DSF), cottonseed meal (CSM), corn steep liquor (CSL), yeast extract (YE), meat extract (ME), peptone (PP), and tryptone (TR). In DSF and CSM, majority of the nitrogen is present in insoluble form, which gets converted to proteins, peptides, and amino acids during fermentation, while in others, the nitrogen is available in the form of proteins, peptides, and free amino acids. Quite often, the outcome of the fermentation is influenced by the distribution of the various forms of nitrogen in the fermentation medium (Aharonowitz and Demain 1979). The regulatory effects of nitrogen substrate on production of secondary metabolites have been reviewed in detail (Aharonowitz 1980; Martin and Demain 1980; Calam 1987; Brana and Demain 1988; Vining and Doull 1988; Sanchez and Demain 2002); however, process models that account for this effect have not been reported.

Although mathematical modeling on carbon catabolite repression is discussed in several papers and reviews (Bajpai and Reuβ 1981; Dynesen et al. 1998; Patnaik 2001), mathematical models describing nitrogen regulation are sparse. Such models can be particularly useful for antibiotic-fed-batch fermentation processes where S_{ONS} is utilized extensively in media formulation as well as during substrate feeding. The rifamycin B antibiotic fermentation represents a typical industrial process where production is "cultivation cost intensive" (Nielsen 1995) and consistent productivities are decisive for profits.

Rifamycin B is a polyketide antibiotic from ansamycin family with a pronounced anti-mycobacterial activity and

P. M. Bapat · S. V. Sohoni · T. A. Moses · P. P. Wangikar
Department of Chemical Engineering,
Indian Institute of Technology,
Bombay, Powai, Mumbai
400 076, India

is extensively used in clinical treatment of tuberculosis, leprosy, and AIDS-related mycobacterial infections (Sepkowitz et al. 1995). Rifamycin B fermentation medium constitutes glucose (S_{Glc}) as a primary carbon source and ammonium sulphate as a nitrogen source. Besides this, fermentation medium also contains soluble and insoluble complex organic nitrogen from DSF and CSL (Sensi and Thiemann 1967). This complex nitrogen provides substitutable carbon and nitrogen to the medium. Sensi and Thiemann (1967) and Venkateswarlu et al. (1999) reported final productivity of rifamycin B with 15 different S_{ONS} in batch fermentation at shake flask level. Kawaguchi et al. (1984) reported a "B factor" from yeast extract as an inducer for rifamycin B synthesis. Despite this information, it remained unclear as to how the organism assimilates this S_{ONS} and whether the form in which the nitrogen is available influences the rifamycin B productivity. El-Tayab et al. (2004) reported on the effect of yeast extract addition at different time points in rifamycin B fermentation but the quantification of nitrogen substrate was not reported.

Earlier, we have reported that media component interactions play an important role in rifamycin B productivity and antibiotic synthesis machinery is sensitive to nitrogen in the form of inorganic as well as organic substrates (Bapat and Wangikar 2004). Further, we have proposed a model that accounts for growth and product formation kinetics of rifamycin B fermentation in a multi-substrate complex medium (Bapat et al. 2006). Here, we present a cybernetic model (Kompala et al. 1984; Dhurjati et al. 1985; Ramkrishna et al. 1997) for rifamycin B fermentation which accounts for the effect of various organic nitrogen sources on rifamycin B productivity. Five different S_{ONS} were chosen based on the form in which nitrogen is available to the organism. We measured some key components representing the available nitrogen in the form of free amino acids and proteins besides regular measurements like biomass, glucose and product. The kinetic data is utilized to develop and validate a process model. The model throws light on some interesting aspects of rifamycin B fermentation that might be useful in developing better media as well as nitrogen substrate feeding strategies.

Materials and methods

Materials

The rifamycin-B-producing strain *A. mediterranei* S699, a gift from Professor Giancarlo Lancini at the former Lepetit Laboratories (Geranzano, Italy), was obtained from Prof. Heinz Floss (Washington University, USA). This strain does not require sodium barbital (Yu et al. 2001). Rifamycin B standard was a gift from Lupin Pharma (Mumbai, India). High-performance liquid chromatography (HPLC) grade water was purchased from Merck (Mumbai, India). Organic nitrogen substrates (ME, YE, PP, and TR) were purchased from Hi-Media (Mumbai, India) and DSF from General Foods (Indore, India).

Methods

Batch fermentation in shake flask

The strain was cultivated and maintained as previously reported (Kim et al. 1996). The seed culture was prepared in 100 ml medium containing glucose as a carbon source. Nitrogen is provided by organic nitrogen substrates like ME, PP, YE, and TR (Bapat and Wangikar 2003). The seed culture was grown for 72 h with a single baffled flask before transferring to the fermentation medium. The fermentation media were composed of micronutrients and glucose as reported previously (Bapat et al. 2006).

Furthermore, the fermentation media was supplemented with one of the S_{ONS} out of YE, ME, TR, PP, and DSF. Care was taken to keep the total initial concentration of nitrogen at 1.5 g l^{-1}; this includes nitrogen from soluble and insoluble components. Inorganic nitrogen substrate was not added in these media. After adjusting the pH to 7.0 with 1 N NaOH, each flask was autoclaved at 121°C for 15 min. Fermentation was initiated by inoculating the fermentation medium with 10% v/v seed culture. Fermentation was carried out in 250-ml flasks with single baffle (working volume 40 ml). Flasks were shaken at 240 RPM at 28°C (Kim et al. 1996). All the fermentation experiments were performed in triplicate.

Analytical techniques

Samples were drawn from the fermentation medium at regular intervals to analyze the concentrations of biomass, glucose, proteins, free amino acids, and rifamycin B. The biomass was measured using pre-weighed filter papers (Whatmann, Brentford, Middlesex, UK) as previously reported (Bapat et al. 2006). The concentration of free amino acids was estimated via the ninhydrin method (Moore 1968). Four milliliters of sample, upon appropriate dilution, was mixed with 1 ml of the ninhydrin reagent containing 10 g l^{-1} of hydrindantin and 20 g l^{-1} ninhydrin. The mixture was boiled for 15 min, and then cooled to room temperature, and the absorbance at 575 nm was measured spectrophotometrically (V-540, Jasco, Tokyo, Japan) to obtain the concentration of free amino acids. Rifamycin B was detected spectrophotometrically (V-540, Jasco, Tokyo, Japan) at a wavelength of 425 nm, as described by Pasqualucci et al. (1970). The rifamycin B concentrations were cross-checked via HPLC for approximately 30% of the samples. For estimating rifamycin B, the broth was mixed 1:1 with butanol and shaked for 4 h at room temperature (150 rpm). After centrifugation (10 min; 5,000×*g*) the butanol phase was separated and 100-µl sample was used for HPLC analysis (Stratmann et al. 2002). Glucose was analyzed via RI detector on HPLC (Hitachi, Merck KgaA, Darmstadt, Germany) using HP-Aminex-87-H column (Biorad, Hercules, CA, USA) at 60°C with a mobile phase of 5 mM sulphuric acid (Ross and Chapital 1987). Protein concentration was determined at 595 nm (V-540, Jasco, Tokyo, Japan) using Bradford reagent with bovine serum albumin as standards (Bradford 1976).

Model description

The model assumes that S_{ONS} is present in two forms, an available form S_{ANS} comprising of amino acids and dipeptides and an unavailable form S_{UNS} such as larger peptides and proteins, both soluble and insoluble. The model further assumes that the organism can grow on (1) S_{ANS} alone with the amino acids acting as sole source of carbon and nitrogen (refer Eq. 1a and 1b for stoichiometry and kinetic expression, respectively) or on (2) S_{Glc} as carbon source and S_{ANS} as a nitrogen source (Eqs. 2a and 2b). The rifamycin B formation takes place with S_{Glc} as a C source and S_{ANS} as N source (Eq. 3a and 3b). Based on our preliminary experiments, we assume that rifamycin B formation does not occur when amino acids are being taken up as sole source of carbon and nitrogen. The nitrogen in the form of S_{UNS} is converted to S_{ANS} via a hydrolytic enzyme X_{E3} (Eqs. 4a and 4b). The model further assumes that the growth and product formation on a specific substrate combination i is dependent on the presence of key enzyme X_{Ei} which may be inducible. The enzyme X_{Ei} is assumed to be synthesized from the cell mass component X (Eq. 5a) with the rate of the enzyme synthesis being dependent on the substrate(s) that are being taken up by X_{Ei} (Eqs. 5b). It is assumed that the synthesis of the proteolytic enzyme X_{E3} (Eqs. 6a) is repressed by the presence of freely available nitrogen (Eq. 6b). The enzymes are assumed to undergo degradation to form components of the cell mass X (Eq. 7a) via first-order kinetics (Eq. 7b). Note that we describe the model in the form of stoichiometric equations and the corresponding kinetic expression as equations a and b, respectively, in Eqs. 1a,b, 2a,b, 3a,b, 4a,b, 5a,b, 6a,b, 7a,b.

Model equations

$$X + Y_{1,3}\mathrm{CO_2} - Y_{1,1}\mathrm{S_{ANS}} - Y_{1,4}\mathrm{O_2} + Y_{1,5}\mathrm{H_2O} = 0 \tag{1a}$$

$$\mu_1 = \mu_1^{\max}\left(\frac{X_{E_1}}{X_{E_1}^{\mathrm{Ref}}}\right) r_1^* \tag{1b}$$

$$X + Y_{2,3}\mathrm{CO_2} - Y_{2,1}\mathrm{S_{ANS}} - Y_{2,2}\mathrm{S_{Glc}} - Y_{2,4}O_2 + Y_{2,5}H_2O = 0 \tag{2a}$$

$$\mu_2 = \mu_2^{\max}\left(\frac{X_{E_2}}{X_{E_2}^{\mathrm{Ref}}}\right) r_2^* \tag{2b}$$

$$P + Y_{3,3}\mathrm{CO_2} - Y_{3,1}\mathrm{S_{ANS}} - Y_{3,2}S_{\mathrm{Glc}} - Y_{3,4}\mathrm{O_2} + Y_{3,5}\mathrm{H_2O} = 0 \tag{3a}$$

$$q_{\mathrm{p}} = q_{\mathrm{p}}^{\max}\left(\frac{X_{E_2}}{X_{E_2}^{\mathrm{Ref}}}\right) r_{2,P}^* \tag{3b}$$

$$S_{\mathrm{ANS}} - S_{\mathrm{UNS}} = 0 \tag{4a}$$

$$r_{\mathrm{diss.}} = \left(\frac{X_{E_3}}{X_{E_3}^{\max}}\right) r_3^* k_3 X \tag{4b}$$

$$X_{E_i} - X = 0 \tag{5a}$$

$$r_{E_i} = k_{E_i} r_i^*;\ \text{For } i = 1, 2 \tag{5b}$$

$$X_{E_3} - X = 0 \tag{6a}$$

$$r_{E_3} = k_{E_3} r_3^* \tag{6b}$$

$$X - X_{E_i} = 0;\ \text{for } i = 1, 2, 3 \tag{7a}$$

$$r_{\mathrm{deg}_i} = k_{\mathrm{deg}_i}\, X_{E_i};\ \text{for } i = 1, 2, 3 \tag{7b}$$

The terms, r_i* in Eqs. 1b, 2b, 3b, 4b, 5b, and 6b represent the effect of substrate limitation on growth and product formation and are given by Eq. 8,

$$\left.\begin{aligned} r_1^* &= \frac{S_{\mathrm{ANS}}}{Ks_{1,1} + S_{\mathrm{ANS}} + \frac{S_{\mathrm{ANS}}^2}{K_{I1,1}}} \\ r_2^* &= \frac{S_{\mathrm{ANS}}}{Ks_{2,1} + S_{\mathrm{ANS}} + \frac{S_{\mathrm{ANS}}^2}{K_{I2,1}}} \quad \frac{S_{\mathrm{Glc}}}{Ks_{2,2} + S_{\mathrm{Glc}} + \frac{S_{\mathrm{Glc}}^2}{K_{I2,2}}} \\ r_{2,P}^* &= \frac{S_{\mathrm{ANS}}}{Kp_{3,1} + S_{\mathrm{ANS}} + \frac{S_{\mathrm{ANS}}^2}{K_{PI3,1}}} \quad \frac{S_{\mathrm{Glc}}}{Kp_{3,2} + S_{\mathrm{Glc}} + \frac{S_{Glc}^2}{K_{PI3,2}}} \\ r_3^* &= \frac{S_{\mathrm{UNS}}}{Ks_{4,1} + S_{\mathrm{UNS}}} \end{aligned}\right\} \tag{8}$$

Finally, the mass balance for biomass (Eq. 9), substrates (Eqs. 10, 11), products (Eq. 12) and enzymes (Eqs. 13 and 14) are given below in the form of differential equations.

$$\frac{dX}{dt} = (\mu_1 + \mu_2)X \tag{9}$$

$$\frac{dS_{Glc}}{dt} = -\left[y_{2,2}\mu_2 + y_{3,2}q_p\right]X \tag{10}$$

$$\frac{dS_{ANS}}{dt} = -\left[y_{1,1}\mu + y_{2,1}\mu_2 + y_{3,1}q_p\right]X + k_3\left(\frac{X_{E_1}}{X_{E_1}^{max}}\right)\left(\frac{S_{UNS}}{ks_{4,1} + S_{UNS}}\right)X \tag{11}$$

$$\frac{dP}{dt} = q_P X \tag{12}$$

$$\frac{d\frac{X_{E_i}}{X_{E_i}\,max}}{dt} = \left(\mu_i^{max} + k_{deg,i}\right)r_i^* - \left(\mu + k_{deg,i}\right)\frac{X_{E_i}}{X_{E_i}\,max};(\text{for } i = 1, 2) \tag{13}$$

$$\frac{d\frac{X_{E_3}}{X_{E_3}\,max}}{dt} = \left(\frac{\mu + k_{deg,3}}{1 + \left(\frac{T_N}{W}\right)^d}\right)r_3^* - \left(\mu + k_{deg,3}\right)\frac{X_{E_3}}{X_{E_3}\,max} \tag{14}$$

Estimation of model parameters

The parameter values were estimated by fitting Eqs. 9, 10, 11 and 12 to the time profiles of the batch data. An analysis of variance (ANOVA) approach to regression analysis is applied, which is based on partitioning the total sum of squares (SSTO) into the error sum of squares (SSE) and regression sum of squares (SSR). In the present study, the parameter values were estimated to obtain best fit between experimental data and model prediction as measured by the R^2 value (Eq. 15). This was achieved by searching the parameter space by using dynamic optimization algorithm 'fmincon' available in Matlab (Mathworks, Natick, MA, USA).

$$R^2 = 1 - \frac{SSE}{SSTO} = \frac{SSR}{SSTO} \tag{15}$$

Where,

(1) $SSTO = \sum\left(Y_i - \overline{Y}\right)^2$; measure of the variation of the observed variables (Y_i) around the mean ($\overline{Y}$).

(2) $SSE = \sum\left(Y_i - \overleftrightarrow{Y_i}\right)^2$; measure of the variation of the observed variables around regression line (Y_i).

(3) $SSR = \sum\left(\overleftrightarrow{Y_i} - \overline{Y}_i\right)^2$; measure of the variation of the fitted regression values around mean.

The routine is utilized to find a constrained maximum of the objective function of several variables such as biomass, rifamycin B, S_{Glc} and S_{ANS}. Note that the stoichiometric coefficients of oxygen, carbon dioxide, and water in Eqs. 1a, 2a, and 3a have not been estimated.

Results

Organic nitrogen substrates, which constitute an important medium component in industrial fermentations, are the byproducts of animal processing and agriculture industry,

Table I Nitrogen distribution in various organic nitrogen sources

Distribution	Yeast extract	Meat extract	Peptone	Tryptone	Soy flour	Reference
Total nitrogen % (w/w)	11.4	13.9	15.4	13.3	11.2	Difco and BBL manual (2003)
Amino nitrogen % (w/w)	6.90	2.0	3.50	5.30	–	Difco and BBL manual (2003)
Concentration of ONS used in the medium[a] (g l^{-1})	13.40	10.79	9.70	8.86	13.39	This study
Calculated N_T° (g l^{-1})	1.50	1.50	1.50	1.50	1.50	This study
Free-amino-acid concentration in the medium[b] (g l^{-1})	4.97	2.34	0.38	1.73	0.13	This study

[a]The concentration of the nitrogen source was chosen to obtain 1.5 g l^{-1} total nitrogen (N_T°) in the initial medium based on the reported total nitrogen % (w/w) present in the S_{ONS}

[b]Free amino acids estimated by drawing as sample from the autoclaved medium before inoculation

Table II Model parameters for growth and rifamycin B formation via *Amycolatopsis mediterranei* S699 on different organic nitrogen substrates

Common parameters														
μ_1^{max} h^{-1}	μ_2^{max} h^{-1}	$Ks_{1,1}$ g l^{-1}	$Ks_{2,2}$ g l^{-1}	$K_{I\ 2,1}$ g l^{-1}	$Y_{1,\ 1}$ g l^{-1}	$Y_{2,\ 1}$ g l^{-1}	$Y_{2,\ 2}$ g l^{-1}	$K_{P\ 3,1}$ g l^{-1}	$K_{PI\ 3,1}$ g l^{-1}	$K_{P\ 3,2}$ g l^{-1}	$K_{PI\ 3,2}$ g l^{-1}	$Y_{3,1}$ g l^{-1}	$Y_{3,2}$ g l^{-1}	$Ks_{4,1}$ g l^{-1}
0.030	0.075	0.01	25	125	0.41	1.70	0.40	0.05	0.60	25	80	1.70	0.30	1.0

and are not completely defined chemically. As a result, batch-to-batch variation is a common problem, which reflects poor reproducibility of productivity. Despite this disadvantage, it is the medium of choice for fermentation industry because of its low cost. Thus, it is of interest to model the effect of S_{ONS} on antibiotic fermentation process.

Previously, we reported a structured model for rifamycin B fermentation in shake flask (Bapat et al. 2006) to predict the growth of *A. mediterranei* S699 on a rifamycin B production. Five different S_{ONS} are chosen. These are commonly used S_{ONS} in fermentation industry from seed development to production stage. The initial concentration of S_{ONS} was chosen such that the total nitrogen load was 1.5 g l^{-1} (Table I). These S_{ONS} substrates differ in their ratio of amino nitrogen to total nitrogen reflecting nitrogen distribution in S_{UNS} and S_{ANS} forms. Even though initial total nitrogen concentration is the same across S_{ONS}, a significant variation is observed in initial S_{ANS} concentration. DSF and PP contain the lowest S_{ANS}, whereas, it is high in YE, TR, and ME.

Parameter estimation and model fit

The experimental data from complex media containing S_{Glc} and ME was used for parameter estimation. The model parameters were obtained by fitting this experimental data to the model using fmincon subroutine from Matlab. The goodness of fit (R^2) for biomass, product, and substrates, calculated from experimental and simulated values, was found to be above 0.90 (Table III). The estimated values of model parameters are listed in Table II. The specific growth rate of the growth on S_{ANS} as the sole source of carbon and nitrogen (μ_1^{max}) was significantly lower than that on S_{ANS} as the N source and S_{Glc} as C source (μ_2^{max}). Furthermore, in preliminary experiment, no product formation was detected when culture was grown on S_{ANS} as sole substrate. This reflects the significance of glucose in rifamycin B production as reported earlier (Bapat et al. 2006). The low values of $Ks_{i,j}$ and $Kp_{i,j}$ for amino acids indicate that growth and product formation can take place even at very low concentration of S_{ANS}. Furthermore, the rifamycin B synthesis is found to be inhibited by S_{ANS} as seen from the low K_{PI} value for amino acids. It is observed that, though model parameters remained same, dissolution contant (k_3) varies from S_{ONS} to S_{ONS} (Table III).

Table III Parameters specific for organic nitrogen substrate

S_{ONS}	k_3 g l^{-1}	R^{2a}
Yeast extract	0.028	0.92
Meat extract	0.032	0.95
Peptone	0.025	0.93
Tryptone	0.026	0.94
Soy flour	0.021	0.90

[a] R^2 is the average coefficient of determination obtained for biomass, glucose, free amino acids, and rifamycin B on different S_{ONS}

The values of X_{Ei}°, the initial level of enzymes, were treated as parameters which needed to be estimated. These were estimated as 0.30, 0.85, and 0.05 for X_{E1}, X_{E2}, and X_{E3}, respectively, with degradation constant ($k_{deg,i}$) of 0.005 h^{-1}. Note that the initial values of enzymes depend on the preculture condition.

Figure 1 shows the comparison of experimental profiles with model simulation. Biomass profile shows short lag phase followed by exponential phase, which lasts for approximately 100 h (Fig. 1a). The glucose consumption starts at the end of lag phase and approximately 10 g l^{-1} glucose remained unutilized at the end of the batch. S_{ANS} utilization starts immediately after inoculation. The S_{UNS} is converted to S_{ANS} to provide a sustained supply of S_{ANS} for growth and product formation. The rifamycin B production starts at 15 h, which is concomitant with simultaneous utilization of S_{Glc} and S_{ANS}. The enzymes X_{E1} and X_{E2} both are at induced level, while X_{E3} is at basal level at the beginning of the batch due to the preculturing condition (Fig. 1c). The amino acid assimilating enzyme X_{E1} gets degraded at around 15 h. At around 45 h X_{E2} synthesis reached its peak level, which was concomitant with the increased activity of X_{E3} enzyme. The growth rate μ_2 reaches its maximum at approximately 30 h and later regulated by S_{ANS} availability via enzyme X_{E3} (Fig. 1d). The rifamycin B production rate (q_p) was inhibited by high concentration of S_{ANS} in the initial phase.

Model validation on complex media

The process model with the estimated parameters was used to predict a priori the growth, product formation, and substrate utilization on other S_{ONS} such as YE, PP, TR, and DSF. Figure 2 shows experimental and predicted profiles on DSF-based complex medium. The model was able to accurately predict the growth, product formation, and substrate uptake.

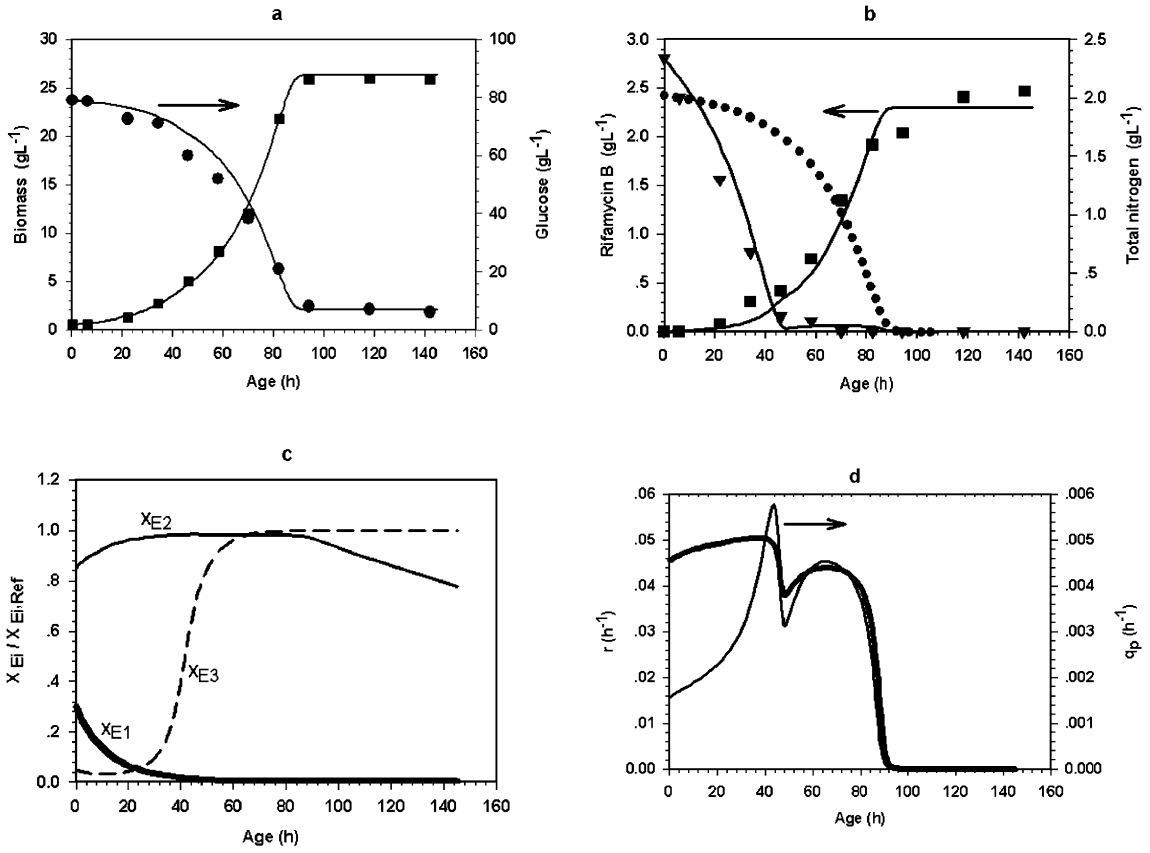

Fig. 1 Rifamycin B fermentation profile in meat-extract-based complex media. Model predictions using cybernetic model (shown as *lines*) as compared to the experimental data. The initial medium contained 80 g l^{-1} glucose, 13.90 g l^{-1} meat extract and other micronutrients. **a** Dry cell weight (g l^{-1})(▪) and glucose concentration (g l^{-1})(•); **b** free amino acid concentration (g l^{-1}) (▾: free amino acids, *dotted line* represents simulated total nitrogen N_T) and rifamycib B (g l^{-1})(▪) ; **c** simulated profiles of key enzymes required for the substrate uptake; **d** simulated profiles of the specific growth rates (h^{-1}) and specific production rates (h^{-1})

The biomass profile is shown in Fig. 2a. Initial growth phase was short with a specific growth rate of 0.04 h^{-1} between 0 and 20 h; later, growth was steady with a specific rate of 0.025 h^{-1} between 20 h and the end of the fermentation. The glucose uptake started at approximately 20 h. A total of 60 g of glucose was utilized during the fermentation (Fig. 2a). In the case of nitrogen (Fig. 2b), the free amino acids (S_{ANS}) were depleted in the first 6 h and later maintained at a pseudo-steady state by the protein hydrolytic enzyme X_{E3}. The rifamycin B production started early at around 15 h and reached a final concentration of 3.5 g l^{-1} at 140 h (Fig. 2b). The model was able to capture the role of insoluble nitrogen and its effect on specific growth and production rates (Fig. 2d). The specific product formation rate remained consistently high as the S_{ANS} was maintained at low concentration by sustained release (Fig. 2d).The growth rate and production rates started decreasing at around 140 h, due to the limiting total nitrogen concentration.

The model was further used to predict growth and production profile on complex media consisting of 80 g l^{-1} S_{Glc} and different organic nitrogen sources. It can be seen that model prediction matches well with the experimental values (Fig. 3). Among the S_{ONS}, glucose consumption is faster in YE with complete utilization of glucose in 90 h. Glucose consumption was slow in TR and PP and approximately 15 g l^{-1} glucose remained unutilized at the end of the fermentation in these two batches. YE contained highest free amino acids (S_{ANS}) at the initiation of fermentation followed by TR and PP. Free amino acids from YE depleted around 50 h, while those in TR and PP depleted much earlier, at 35 h and 20 h, respectively. The rifamycin B production rate showed significant lag in TR, YE, and ME (Fig. 3d). The increase in production rate was concomitant with the decrease in free amino acid concentration in YE- and TR-based complex media. In PP, rifamycin B synthesis started from the initiation of the batch. In PP-based complex media, production rate was high at round 0.006 h^{-1} for the first 20 h. Later, the rate dropped and remained steady at 0.004 h^{-1}.

The model is able to predict the variations in the rifamycin production rates caused by variation in S_{ANS}/S_{UNS} ratio in the different organic nitrogen sources. For example, due to the low S_{ANS} concentration, production rate q_p reaches its highest value (0.0065 h^{-1}) in S_{ONS} such as PP and DSF at the beginning of the fermentation (Fig. 3d) and later maintained at around 0.005 h^{-1} through sustained release of S_{ANS} from S_{UNS}. The production rate is

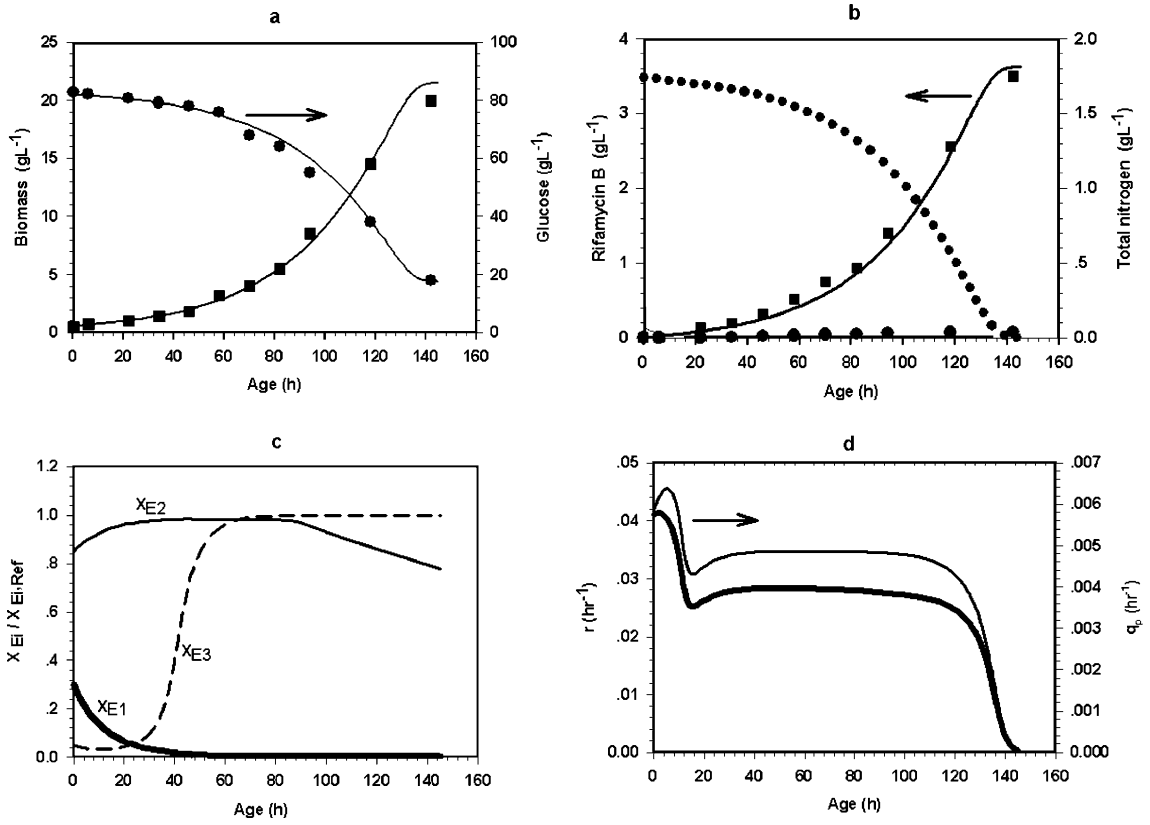

Fig. 2 Cybernetic model predictions for low S_{ANS} containing organic nitrogen substrate, defatted soy flour. Model predictions using cybernetic model (shown as *lines*) as compared to the experimental data. The initial medium contained 80 g l^{-1} glucose, 13.40 g l^{-1} soy flour and other micronutrients. **a** to **d** Refer legend to Fig. 1

severely inhibited in other S_{ONS}. The inhibition is highest in YE, followed by that in TR and ME. Although the production rate reaches its peak value in other S_{ONS}, it drops quickly. The model developed here is, thus, able to capture the changes in the rate profile based on the form in which nitrogen is available in these S_{ONS}.

Discussion

It is common to use organic nitrogen substrates in industrial fermentation media, as this is much cheaper than other nitrogen substrates. The disadvantage is the heterogeneity and the irreproducible productivity generally associated with these complex organic nitrogen substrates. Further, the free amino acid concentration in the organic nitrogen source have a significant impact on productivity, as high values may inhibit/repress the biosynthesis of antibiotic, and very low values may be limiting for the desired biosynthesis (Untrau et al. 1994). Balancing nitrogen in the form of S_{ANS}/S_{UNS} ratio is a challenge, as in ideal fermentation medium, rapid growth is desirable in the initial phase, followed by a production phase. Thus, it is of interest to develop a model which can predict the possible role of S_{ANS} on antibiotic productivity. The model presented in this paper is able to predict growth and product formation on different S_{ONS}. We model this by partitioning S_{ONS} into available nitrogen substrate(S_{ANS}) and unavailable nitrogen substrate (S_{UNS}). To the best of our knowledge, this is the first report where a unified model is applicable to different S_{ONS} substrates. The model is based on cybernetic principles where an organism is assumed to invest its resources on the substrates which supports the highest growth.

A total of five different S_{ONS} were used for estimation and validation of model parameters. We observed that productivities differ significantly in these S_{ONS} despite total nitrogen load being comparable. The model is able to explain this, based on the amino acid formation and utilization rates. It is observed that organism starts converting S_{UNS} to S_{ANS} after depletion of initial free amino acids present in the medium. The initiation of this transition phase differs from S_{ONS} to S_{ONS}. With YE, this transition occurs late at around 45 h, whereas, in DSF it starts early at around 6 h. This phase is very crucial for rifamycin B production as the growth and production rates solely depend on the availability of S_{ANS}. In S_{ONS} such as YE, ME, and TR, high concentration of S_{ANS} resulted in rapid growth but failed to support high growth rate due to the limiting pool of S_{UNS}. In S_{ONS} like PP, the low

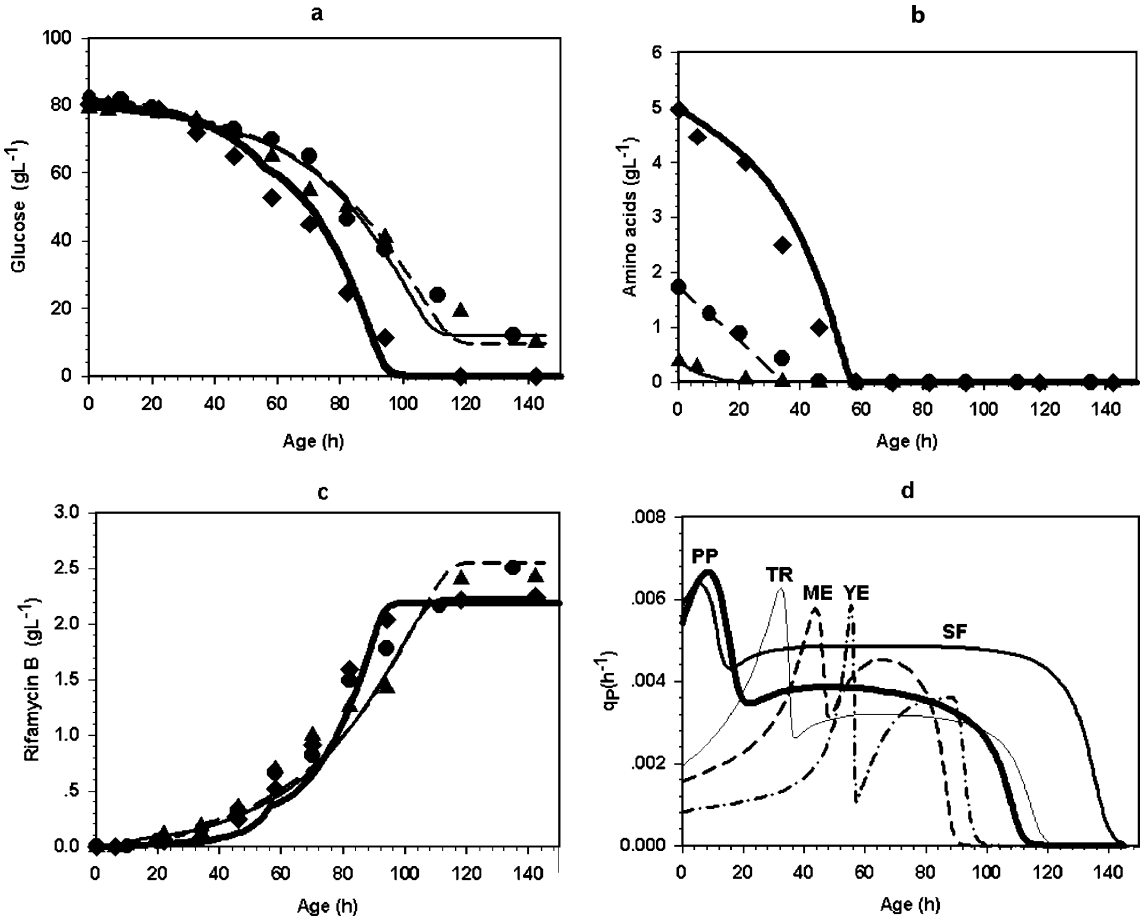

Fig. 3 Prediction of cybernetic model on other S_{ONS}. Model predictions using cybernetic model (shown as *lines*) as compared to the experimental data. Different S_{ONS} were sterilized with media containing 80 g l^{-1} glucose, 11 g l^{-1} $CaCO_3$, 1 g l^{-1} KH_2PO_4, 1 g l^{-1} $MgSO_4$, 0.01 g l^{-1} FeSO4, 0.05 g l^{-1} $ZnSO_4$, 0.003 g l^{-1} $CoCl_2$.. ♦Yeast extract; • tryptone; ▲ peptone. *Continuous lines* represent cybernetic model prediction. **a** Glucose concentration (g l^{-1}); **b** free amino acid concentration (g l^{-1}); **c** rifamycin B concentration (g l^{-1}); **d** production rates (h^{-1}). For initial concentration of these S_{ONS}, refer to Table 1

concentration of S_{ANS} did not affect rapid growth and can be seen from dextrose-utilization profile which is similar to that of TR and ME. DSF is an extreme case where the process of S_{UNS} to S_{ANS} depends on the rate of dissolution of insoluble matter into media and conversion of the same in S_{ANS}. Glucose consumption rate is lowest in this batch. These results indicate that availability of S_{ANS} depends on the nature of S_{ONS}.

The rifamycin B synthesis seems to depend on the ratio of S_{ANS}/S_{UNS}. In the DSF- and PP-based media where the ratio is low, the production rate is high from the beginning of the batch, whereas, it is low in other S_{ONS}, where the S_{ANS}/S_{UNS} ratio is high. The model is able to predict this effect successfully.

The model presented in this paper can be utilized in model-based optimization of initial media composition and substrate feed strategy and in monitoring the fermentation process. The modeling results would be of specific interest to the scientific community working with actinomycetes, while the modeling strategy would be useful for modeling other industrial fermentations that employ complex media.

References

Aharanowitz Y (1980) Nitrogen metabolite regulation of antibiotic biosynthesis. Annu Rev Microbiol 34:9–33

Aharanowitz Y, Demain AL (1979) Nitrogen nutrition and regulation of cephalosporin production in *Streptomyces clavuligerus*. Can J Microbiol 25:61–67

Bajapai RK, Reuß M (1981) Evaluation of feeding strategies in carbon regulated secondary metabolite production through mathematical modeling. Biotechnol Bioeng 23:739–763

Bapat PM, Wangikar PP (2004) Optimization of Rifamycin B fermentation in shake flasks via a machine-learning-based approach. Biotechnol Bioeng 86:201–208

Bapat PM, Kundu S, Wangikar PP (2003) An optimized method for *Aspergillus niger* spore production on natural carrier substrates. Biotech Prog 19:1683–1688

Bapat PM, Nandy S, Wangikar P, Venkatesh KV (2005) Quantification of metabolically active biomass using Methylene Blue dye Reduction Test (MBRT): measurement of CFU in about 200 s. J Microbiol Methods DOI 10.1016/j.mimet.2005.06.010

Bapat PM, Bhartiya S, Venkatesh KV, Wangikar PP (2006) A structured kinetic model to represent the utilization of multiple substrates in complex media during rifamycin B fermentation. Biotechnol Bioeng DOI 10.1002/bit.20767

Bascaran V, Hardisson C, Brana A (1989) Regulation of nitrogen catebolite enzymes in *Streptomyces clavuligerus*. J Gen Microbiol 135:2465–2474

Bradford MM (1976) A rapid and sensitive method for the quantitation of microgram quantities of protein utilizing the principle of protein dye binding. Anal Biochem 72:248–254

Brana AF, Demain AL (1988) Nitrogen control of antibiotic biosynthesis in actinomycetes. In: Sanchez SE, Boca RFL (eds) Nitrogen source control of microbial processes. CRC, London, UK, pp 99–119

Calam CT (1987) Process development in antibiotic fermentations. University of Cambridge, Cambridge, pp 1–217

Dhurjati P, Ramkrishna D, Flickinger MC, Tsao GT (1985) A cybernetic view of microbial growth: modeling of cells as optimal strategists. Biotechnol Bioeng 27:1–9

Dynesen J, Smits HP, Olsson L, Nielsen J (1998) Carbon catabolite repression of invertase during batch cultivations of *Saccharomyces cerevisiae*: the role of glucose, fructose, and mannose. Appl Microbiol Biotechnol 50:579–582

El-Tayeb OM, Salama AA, Hussein MMM, El-Sedawy HF (2004) Optimization of industrial production of rifamycin B by *Amycolatopsis mediterranei.* I. The role of colony morphology and nitrogen sources in productivity. Afr J Biotechnol 3:266–272

Kawahuchi T, Asahi T, Satoh T, Uozumi T, Beppu T (1984) B factor, an essential regulatory substance inducing the production of rifamycin in *Nocardia* sp. J Antibiotics 37:1587–1595

Kim CG, Kirschning A, Bergon P, Zhou P, Su E, Sauerbrei B, Ning S, Ahn Y, Breuer M, Leistner E (1996) Biosynthesis of 3-amino-5-hydroxybenzoic acid, the precursor of mC(7)N units in ansamycin antibiotics. JACS 118:7486–7491

Kompala DS, Ramakrishna D, Tsao GT (1984) Cybernetic modelling of microbial growth in simple substrates. Biotechnol Bioeng 26:1272–1281

Krabben P, Theodorus D (2001) Fermentation process to produce clavulanic acid at a low concentration of free amino acids. WO Patent 00/01840

Martin JF, Demain AL (1980) Control of antibiotic synthesis. Microbiol Rev 44:230–251

Moore S (1968) Amino acid analysis: aqueous dimethyl sulfoxide as solvent for the ninhydrin reaction. J Biol Chem 243:6281–6283

Nielsen J (1995) Physiological engineering aspect of *Penicillium chrysogenum*. Polyteknisk Forlag, Lingby, Denmark

Pasqualucci CR, Radaelli P, Gallo GG (1970) Improved differential spectrophotometric determination of rifamycins. J Pharm Sci 59:685–687

Patnaik PR (2001) Penicillin fermentation: mechanisms and models for industrial-scale bioreactors. Crit Rev Microbiol 27:25–39

Ramakrishna R, Ramkrishna D, Konopka AE (1997) Microbial growth on substitutable substrates: characterizing the consumer–resource relationship. Biotechnol Bioeng 54:77–90

Ross LF, Chapital DC (1987) Simultaneous determination of carbohydrates and products of carbohydrate metabolism in fermentation mixtures by HPLC. J Chromatogr Sci 25:112–117

Sanchez S, Demain AL (2002) Metabolic regulation of fermentation process. Enzyme Microbiol Technol 31:895–906

Sensi P, Thiemann JE (1967) Production of rifamycins. Prog Ind Microbiol 6:21–59

Sepkowitz KA, Rafalli J, Riley L, Kiehn TE, Armstrong D (1995) Tuberculosis in the AIDS era. Clin Microbiol Rev 8:180-199

Stanbury PF, Whitaker A (1984) The development of inocula for industrial fermentations. In: Principles of fermentation technology. Oxford Pergamon, pp 108–119

Stratmann A, Schupp T, Toupet C, Schilling W, Oberer L, Traber R (2002) New insights into rifamycin B biosynthesis: isolation of proansamycin B and 34a-deoxy-rifamycin W as early macrocyclic intermediates indicating two separated biosynthetic pathways. J Antibiotics 55:396–406

Untrau S, Lebrihi A, Lefebvre G, Germain P (1994) Nitrogen catebolite regulation of Spiramycin production in *Streptomyces ambofaciens*. Curr Microbiol 28:111–118

Venkateswarlu G, Murali Krishna PS, Rao VL (1999) Production of rifamycin using *Amycolatopsis mediterranei* (MTCC14). Bioprocess Eng 20:27–30

Vining LC, Doull JL (1988) Catebolite repression of secondary metabolism in actinomycetes. In: Okami M (eds) 7th International symposium on Biology of Actinomycetes. Japan Scientific Societies, Tokyo, pp 406–411

Yu TW, Muller R, Muller M, Zhang XH, Draeger G, Kim CG, Leistner E, Floss HG (2001) Mutational analysis and reconstituted expression of the biosynthetic genes involved in the formation of 3-amino-5-hydroxybenzoic acid, the starter unit of rifamycin biosynthesis in *Amycolatopsis mediterranei* S699. J Biol Chem 276:12546–12555

Zimbro MJ, Power DA (2003) (eds) Difco and BBL manual of microbiological culture media. Becton, Dickinson and company, Maryland, USA, pp 686–687